Self-Powered p-GaN/i-$ZnGa_2O_4$/n-ITO Heterojunction Broadband Ultraviolet Photodetector With High Working Temperature

Yongxue Zhu, Kewei Liu, *Member, IEEE*, Xiaoqian Huang, Peixuan Zhang, Qiu Ai, Zhen Cheng, Jialin Yang, Xing Chen, Binghui Li, Lei Liu, and Dezhen Shen

***Abstract*— A self-driven p-GaN/i-$ZnGa_2O_4$/n-ITO heterojunction broadband ultraviolet (BUV) photodetector was firstly demonstrated in this work with a high working temperature. In the 25-300 °C temperature range, the device exhibits excellent and stable BUV photodetection performance. Even at 300 °C, a large peak responsivity of ∼132 mA/W, a broad UV response band ranging from 250 to 400 nm, a high UV-to-visible rejection ratio of nearly 10^4, and a high −3 dB cutoff frequency of 20 kHz can be still observed at 0 V, which is obviously superior to the other reported high-temperature BUV heterojunction photodetectors. The remarkable performance of our device at high temperature can be attributed to the excellent insulation and high crystalline quality of i-$ZnGa_2O_4$ layer, as well as the good electrical properties of p-GaN and n-ITO. Moreover, their wide and complementary band gaps make the device have a very broad UV detection band.**

***Index Terms*— Broadband ultraviolet photodetector, heterojunction, high-temperature, self-powered, $ZnGa_2O_4$.**

I. Introduction

BROADBAND ultraviolet (BUV) photodetectors (PDs) have drawn significant attention in recent years because of their wide applications in flame detection, space exploration, missile plume detection, environmental and biological research [1], [2], [3], [4]. Since many applications require stable devices capable of working at high temperature, it is obviously necessary and important to realize thermally stable PDs [5], [6], [7], [8], [9], [10]. Benefiting from the complementary band gaps, the heterojunction PDs provide a huge potential for broadband detection [11], [12]. Moreover, the built-in electric field at the heterojunction interface could effectively separate the photo-generated carriers, allowing the device to work without external bias [13], [14], [15]. Because no additional bias voltage is required, the heterojunction detector in self-driven operation mode could be completely free from the restriction of dark current when operating at high temperature. Therefore, the self-powered heterojunction PDs formed from different wide-bandgap semiconductor materials, such as, r-GO/HR-GaN [2], β-Ga_2O_3/4H-SiC [16], Ga_2O_3/ZnO [17], diamond/β-Ga_2O_3 [18], Graphene/$(AlGa)_2O_3$/GaN [19], and so on, have become ideal candidates for preparing BUV devices that can meet the requirements of high-temperature applications. Although numerous excellent heterojunction devices have been demonstrated with broadband UV response and zero power consumption, the device performance often deteriorates rapidly as the operating temperature increases [2], [17], [19], [20]. The main reason for this phenomenon is that almost all the reported BUV heterojunction devices are based on simple p-n or n-n structures. With the increase of operating temperature, the ionization rates of the p- and n-layers increase, leading to the narrowing of the depletion region, which would reduce the quantity of photo generated carriers in it.

Compared with p-n heterostructure, p-i-n heterojunction has special advantages, such as higher responsivity, faster response speed and higher reliability, thus allowing higher operating temperature [21], [22], [23], [24], [25]. In this work, a self-driven BUV PD, which still has excellent optoelectronic detection capability even at 300 °C, has been demonstrated for the first time on p-GaN/i-$ZnGa_2O_4$/n-ITO heterojunction. P-GaN, i-$ZnGa_2O_4$ and n-ITO with band gap energies of 3.40, 5.10 and 3.85 eV at room temperature were fabricated by molecular beam epitaxy (MBE), metal organic chemical vapor deposition (MOCVD) and radio-frequency magnetron sputtering, respectively.

Benefitting from the good crystalline quality and excellent insulation of i-$ZnGa_2O_4$ layer and high electrical conductivity

Manuscript received 21 March 2023; accepted 26 March 2023. Date of publication 29 March 2023; date of current version 26 April 2023. This work was supported in part by the National Natural Science Foundation of China under Grant 62074148, Grant 11727902, and Grant 12204474; and in part by the National Ten Thousand Talent Program for Young Top-Notch Talents and Youth Innovation Promotion Association, Chinese Academy of Sciences (CAS), under Grant 2020225. The review of this letter was arranged by Editor T.-Y. Seong. *(Corresponding author: Kewei Liu.)*

Yongxue Zhu, Qiu Ai, Zhen Cheng, and Jialin Yang are with the State Key Laboratory of Luminescence and Applications, Changchun Institute of Optics, Fine Mechanics and Physics, Chinese Academy of Sciences, Changchun 130033, China.

Kewei Liu, Xiaoqian Huang, Peixuan Zhang, Xing Chen, Binghui Li, Lei Liu, and Dezhen Shen are with the State Key Laboratory of Luminescence and Applications, Changchun Institute of Optics, Fine Mechanics and Physics, Chinese Academy of Sciences, Changchun 130033, China, and also with the Center of Materials Science and Optoelectronics Engineering, University of Chinese Academy of Sciences, Beijing 100049, China (e-mail: liukw@ciomp.ac.cn).

Color versions of one or more figures in this letter are available at https://doi.org/10.1109/LED.2023.3262755.

Digital Object Identifier 10.1109/LED.2023.3262755

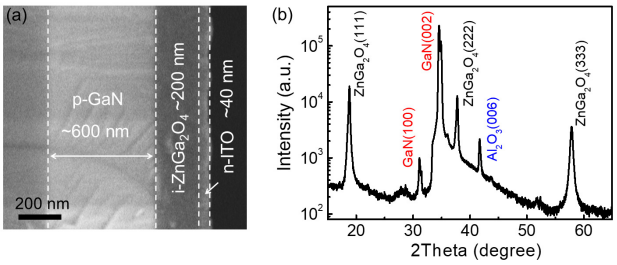

Fig. 1. (a) Side-view SEM image and (b) ω-2θ scanning pattern of the p-GaN/i-$ZnGa_2O_4$/n-ITO heterojunction.

of p-GaN and n-ITO, our p-i-n heterojunction device can work in a wide temperature range with excellent performance. At 300 °C, the device shows a broad UV response band ranging from 250 to 400 nm, a high peak responsivity (R_{peak}) of ~132 mA/W at 352 nm, UV-to-visible rejection ratio of nearly 10^4, and a high −3 dB cutoff frequency of 20 kHz.

II. Material Epitaxy and Device Fabrication

The Mg-doped p-GaN film was firstly grown on undoped GaN (u-GaN)/sapphire template at 750 °C by MBE. During growth, the N_2 flow rate was fixed at 1.8 sccm with radio frequency power of 350 W, and the temperatures of Mg and Ga cells were controlled at 343 and 1120 °C, respectively. Subsequently, i-$ZnGa_2O_4$ film was deposited on the p-GaN layer by MOCVD. Diethylzinc and trimethylgallium with high purity nitrogen as carrier gas and 5N-purity O_2 were employed as Zn, Ga and O sources, respectively. The chamber pressure was kept at 23 Torr and the substrate temperature was maintained at 650 °C. After that, n-type indium tin oxide (ITO) was fabricated on i-$ZnGa_2O_4$ layer by radio-frequency magnetron sputtering. Ni/Au (~50/50 nm) and In (~100 nm) have been used as the ohmic contact electrodes to p-GaN and n-ITO, respectively.

The material characterization was performed by a scanning electron microscope (SEM) (HITACHI S-4800), a Bruker D8GADDS X-ray diffractometer (XRD), a Lakeshore Hall effect measurement system and an UV-3101PC scanning spectrophotometer. Agilent B1500A semiconductor device analyzer was used to measure the time-dependent current (I-t) and current-voltage (I-V) curves. 310 nm light was produced by light emitting diode (LED). A monochromator with a UV-enhanced Xe lamp (200 W) was used to measure the spectral response of the device.

III. Results and Discussion

Fig. 1a presents the side-view SEM image of the p-GaN/i-$ZnGa_2O_4$/n-ITO heterojunction. The thickness of n-ITO, i-$ZnGa_2O_4$ and p-GaN layers can be estimated to be about 40 nm, 200 nm and 600 nm, respectively. Fig. 1b shows the ω-2θ scanning patterns of p-i-n heterojunction prepared on u-GaN/sapphire template. Besides the sapphire substrate diffraction peak, the peaks at $2\theta = 31.1°$ and 34.6° can be respectively attributed to the (100) and (002) planes of GaN. And the diffraction peaks located at 18.85°, 37.56°, and 57.48° can be assigned to the (111), (222), and (333) crystal facets of $ZnGa_2O_4$, respectively [26]. The strong and narrow diffraction

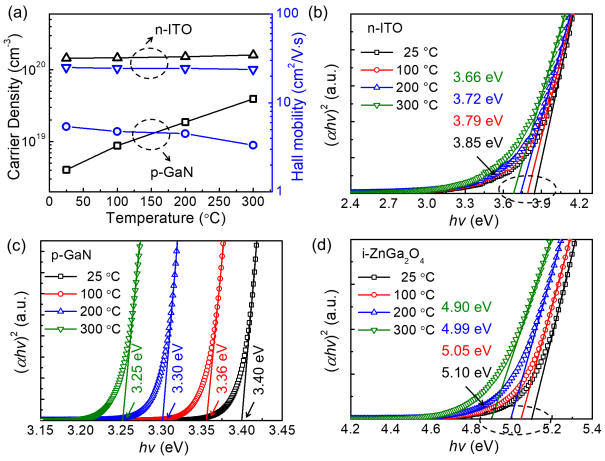

Fig. 2. (a) Carrier density and mobility of p-GaN and n-ITO layers versus temperature. $(\alpha h\nu)^2$ as a function of ($h\nu$) of (b) n-ITO, (c) p-GaN and (d) i-$ZnGa_2O_4$ layers at different temperatures.

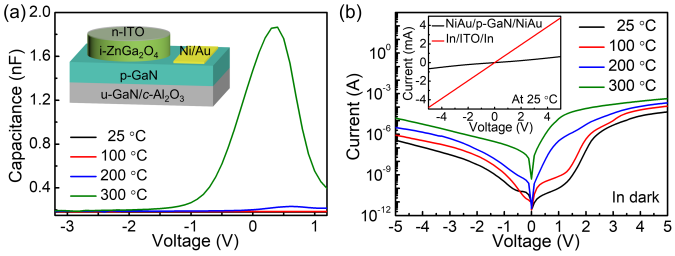

Fig. 3. (a) C–V, and (b) I–V characteristics of the p-GaN/i-$ZnGa_2O_4$/n-ITO heterojunction at different temperatures. The insets of (a) and (b) are the schematic device structure and the I–V characteristics of In/n-ITO and NiAu/p-GaN contacts, respectively.

peaks in XRD pattern indicate that both p-GaN and i-$ZnGa_2O_4$ have good crystalline quality.

To research the optical and electrical properties, optical absorption measurements and Hall effect were carried out at various temperatures of 25, 100, 200, and 300 °C (see Fig. 2) The hall mobility and carrier density of p-GaN layer were measured to be ~5.4 cm^2/Vs and ~4.0 × 10^{18} /cm^3 at 25 °C. With the increase of temperature, the ionization rate of acceptor impurity increases, leading to the increase in hole concentration. At the same time, Hall mobility decreases with increasing temperature. In contrast, the electron concentration and mobility of n-ITO at different temperatures were similar, which can be estimated to be ~1.4 × 10^{20} /cm^3 and ~25 cm^2/Vs. Variation of $(\alpha h\nu)^2$ versus the photo energy ($h\nu$) of n-ITO, p-GaN and i-$ZnGa_2O_4$ under various temperatures are shown in Fig. 2b, 2c and 2d, respectively. The band gaps of ITO (3.85 eV at 25 °C), GaN (3.40 eV at 25 °C) and $ZnGa_2O_4$ (5.10 eV at 25 °C) narrow with increasing temperature, and decrease by 0.19 eV, 0.15 eV and 0.20 eV from 25 to 300 °C, respectively.

To further investigate the photodetection performance, a cylindrical p-GaN/i-$ZnGa_2O_4$/n-ITO heterojunction device with a diameter of ~0.66 mm was fabricated (inset of Fig. 3a). The quasi-linear I–V curves (inset of Fig. 3b) of In/n-ITO/In and NiAu/p-GaN/NiAu indicate that both p- and n-type contacts are Ohmic in nature. C-V characteristics of the device are characterized at different temperatures as shown in Fig. 3a.

TABLE I
COMPARISON TABLE FOR SELF-POWERED HETEROJUNCTION HIGH-TEMPERATURE UV PDS

Device structure	Temperature range	Response band (10% of R_{peak}, nm)	Peak responsivity (A/W)	Rise/decay time	UV/visible rejection ratio	Ref
r-GO/HR-GaN	25-116 °C	250-360	~4.6×10^{-5} (340 nm, 25 °C)	~15/~18 ms (25 °C)	~2×10^{2} (25 °C)	[2]
β-Ga_2O_3/4H-SiC	25-500 °C	210-340	~0.053 (260 nm, 25 °C)	~30/~30 μs (25 °C)	~10^{4} (25 °C)	[16]
ϵ-Ga_2O_3/ZnO	25-327 °C	230-280	~2×10^{-4} (254 nm, 327 °C)	~0.2/~0.1 s (327 °C)	—	[17]
Graphene/$(AlGa)_2O_3$/GaN	25-180 °C	180-260	~0.02 (210 nm, 25 °C)	(t_d) ~10 ms (25 °C)	~10^{4} (25 °C)	[19]
Pt/$ZnGa_2O_4$/p-Si	25-200 °C	240-300	~1.36×10^{-3} (258 nm, 25 °C)	(t_d) ~50 ms (25 °C)	~10^{5} (25 °C)	[27]
p-GaN/i-$ZnGa_2O_4$/n-ITO	25-300 °C	250-400	~0.132 (352 nm, 300 °C)	~13/~14 μs (300 °C)	~10^{4} (300 °C)	This work

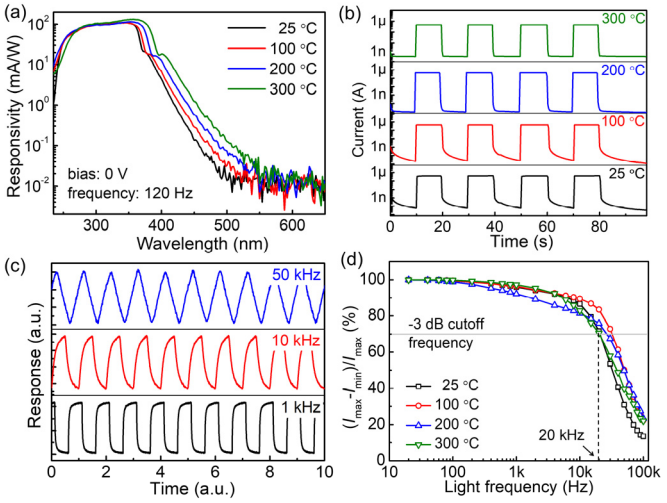

Fig. 4. (a) Spectral response and (b) time-dependent current measured from 25 to 300 °C under 0 V applied bias. (c) Temporal photo response (at 300 °C) under the modulated light of a 310 nm LED. (d) $(I_{max} - I_{min})/I_{max}$ versus illumination modulation frequency under various temperatures.

At 0 V, the capacitance of the detector is about 180 pF at 25 °C, 184 pF at 100 °C, 200 pF at 200 °C, and 1.47 nF at 300 °C.

Below 200 °C, the capacitance of the device almost does not change with the bias voltage, indicating that i-$ZnGa_2O_4$ layer has been completely depleted. When the temperature rises to more than 200 °C, impurities in i-$ZnGa_2O_4$ layer would be ionized, leading to a slight narrowing of the space charge region, which further results in the increase of capacitance. Fig. 3b presents the dark *I-V* curves of the p-i-n PD at different temperatures and clear rectification characteristics can be acquired.

Fig. 4a shows the spectral response measured from 25 to 300 °C under 0 V bias. A broadband UV photoresponse (10% of R_{peak}) ranging from 250 to 400 nm can be clearly observed at all temperatures. According to the experimental band gaps of three semiconductors in our device (ITO: 3.85 eV, $ZnGa_2O_4$: 5.10 eV, GaN: 3.40 eV), the response in the UVA/UVB region should be mainly attributed to p-GaN and n-ITO layers, while the response in UVC region is mainly associated with i-$ZnGa_2O_4$ layer. Additionally, with increasing the temperature, the long-wavelength cut-off edge determined by p-GaN layer shifted towards the longer wavelength region due to the decrease of the band gap. At 300 °C, the peak responsivity at 352 nm is as high as 132 mA/W, and a high UV-to-visible rejection nearly 10^4 was obtained. To further study the response speed characteristics, the *I-t* curve was measured by turning ON/OFF a 310 nm LED (0.768 mW/cm^2) under various temperatures at 0 V (see Fig. 4b). Obviously, the device presents an excellent ON/OFF switching property with fast speed, good reproducibility and high stability at all temperatures. Due to the self-powered operating mode, the device maintains a high ON/OFF current ratio of more than 10^3 at 300 °C. To further estimate the response speed, the normalized temporal response (at 300 °C) of the device were measured at 0 V by oscilloscope under 310 nm modulated LED illumination with different modulation frequency (see Fig. 4c). And the rise and decay times can be estimated to be about 13 μs and 14 μs, respectively. Even at frequencies up to 50 kHz, the device still maintains good optoelectronic detection capability. Fig. 4d plots the relative balance $(I_{max}-I_{min})/I_{max}$ as a function of illumination modulation frequency at different temperatures, where I_{min} and I_{max} are the minimum and maximum current obtained by switching ON/OFF 310 nm light at each frequency. As the modulation frequency increases, the relative balance gradually decreases, and the −3 dB cutoff frequency of the detector exceeds 20 kHz at all temperatures (see Fig. 4d).

Some key parameters of the high-temperature self-powered heterojunction PDs were summarized in Table I. It can be seen that our device has the fastest response, the widest response band and the largest responsivity speed at high temperature. In fact, most of the reported devices have only observed the UV response at high temperature, while the detailed performance parameters are rarely studied. The high crystalline quality and excellent insulation of i-$ZnGa_2O_4$ layer, as well as the good electrical properties of p-GaN and n-ITO could account for the superior photodetection performance of our device at high temperature. Moreover, their wide and complementary band gaps enable the broadband UV detection.

IV. CONCLUSION

In summary, a high-temperature self-powered heterojunction BUV PD was demonstrated based on p-GaN/i-$ZnGa_2O_4$/n-ITO structure. Benefitting from the excellent insulation of i-$ZnGa_2O_4$ layer, good electrical properties of p-GaN and n-ITO, and their wide and complementary band gaps, the p-i-n heterojunction PD shows a high peak responsivity of ~132 mA/W, a broad UV response band ranging from 250 to 400 nm, a high UV-to-visible rejection ratio of nearly 10^4 and a high −3 dB cutoff frequency of 20 kHz at 300 °C. The result reported in this letter provides a feasible way for developing BUV PDs with high operating temperature.

REFERENCES

[1] T. He, X. Zhang, X. Ding, C. Sun, Y. Zhao, Q. Yu, J. Ning, R. Wang, G. Yu, S. Lu, K. Zhang, X. Zhang, and B. Zhang, "Broadband ultraviolet photodetector based on vertical Ga_2O_3/GaN nanowire array with high responsivity," *Adv. Opt. Mater.*, vol. 7, no. 7, Apr. 2019, Art. no. 1801563, doi: 10.1002/adom.201801563.

[2] N. Prakash, G. Kumar, M. Singh, S. P. Singh, B. Satpati, S. P. Khanna, and P. Pal, "Long-term, high-voltage, and high-temperature stable dual-mode, low dark current broadband ultraviolet photodetector based on solution-cast R-GO on MBE-grown highly resistive GaN," *Adv. Opt. Mater.*, vol. 7, no. 18, Sep. 2019, Art. no. 1900340, doi: 10.1002/adom.201900340.

[3] A. Kalra, S. Vura, S. Rathkanthiwar, R. Muralidharan, S. Raghavan, and D. N. Nath, "Demonstration of high-responsivity epitaxial β-Ga_2O_3/GaN metal–heterojunction-metal broadband UV–A/UV-C detector," *Appl. Phys. Exp.*, vol. 11, no. 6, Jun. 2018, Art. no. 064101, doi: 10.7567/apex.11.064101.

[4] P. Li, H. Shi, K. Chen, D. Guo, W. Cui, Y. Zhi, S. Wang, Z. Wu, Z. Chen, and W. Tang, "Construction of GaN/Ga_2O_3 p–n junction for an extremely high responsivity self-powered UV photodetector," *J. Mater. Chem. C*, vol. 5, no. 40, pp. 10562–10570, 2017, doi: 10.1039/c7tc03746e.

[5] H.-T. Zhou, L.-J. Cong, J.-G. Ma, M.-Z. Chen, D.-Y. Song, H.-B. Wang, P. Li, B.-S. Li, H.-Y. Xu, and Y.-C. Liu, "High-performance high-temperature solar-blind photodetector based on polycrystalline Ga_2O_3 film," *J. Alloys Compounds*, vol. 847, Dec. 2020, Art. no. 156536, doi: 10.1016/j.jallcom.2020.156536.

[6] B. R. Tak, M. Garg, S. Dewan, C. G. Torres-Castanedo, K.-H. Li, V. Gupta, X. Li, and R. Singh, "High-temperature photocurrent mechanism of β-Ga_2O_3 based metal-semiconductor-metal solar-blind photodetectors," *J. Appl. Phys.*, vol. 125, no. 14, Apr. 2019, Art. no. 144501, doi: 10.1063/1.5088532.

[7] M. Angelone, N. Fonnesu, M. Pillon, G. Prestopino, F. Sarto, E. Milani, M. Marinelli, C. Verona, and G. Verona-Rinati, "Spectrometric performances of monocrystalline artificial diamond detectors operated at high temperature," *IEEE Trans. Nucl. Sci.*, vol. 59, no. 5, pp. 2416–2423, Oct. 2012, doi: 10.1109/tns.2012.2210735.

[8] A. Metcalfe, G. R. Fern, P. R. Hobson, T. Ireland, A. Salimian, J. Silver, D. R. Smith, G. Lefeuvre, and R. Saenger, "Development of high temperature, radiation hard detectors based on diamond," *Nucl. Instrum. Methods Phys. Res. A, Accel. Spectrom. Detect. Assoc. Equip.*, vol. 845, pp. 128–131, Feb. 2017, doi: 10.1016/j.nima.2016.06.091.

[9] X. Sun, Z. Wang, H. Gong, X. Chen, Y. Zhang, Z. Wang, X. Yu, F. Ren, H. Lu, S. Gu, Y. Zheng, R. Zhang, and J. Ye, "M-plane α-Ga_2O_3 solar-blind detector with record-high responsivity-bandwidth product and high-temperature operation capability," *IEEE Electron Device Lett.*, vol. 43, no. 4, pp. 541–544, Apr. 2022, doi: 10.1109/led.2022.3156177.

[10] N. Watanabe, T. Kimoto, and J. Suda, "4H-SiC pn photodiodes with temperature-independent photoresponse up to 300 °C," *Appl. Phys. Exp.*, vol. 5, no. 9, Sep. 2012, Art. no. 094101, doi: 10.1143/apex.5.094101.

[11] C. Xie, P. You, Z. Liu, L. Li, and F. Yan, "Ultrasensitive broadband phototransistors based on perovskite/organic-semiconductor vertical heterojunctions," *Light, Sci. Appl.*, vol. 6, no. 8, Feb. 2017, Art. no. e17023, doi: 10.1038/lsa.2017.23.

[12] P. Wang, S. Liu, W. Luo, H. Fang, F. Gong, N. Guo, Z.-G. Chen, J. Zou, Y. Huang, X. Zhou, J. Wang, X. Chen, W. Lu, F. Xiu, and W. Hu, "Arrayed van der Waals broadband detectors for dual-band detection," *Adv. Mater.*, vol. 29, no. 16, Apr. 2017, Art. no. 1604439, doi: 10.1002/adma.201604439.

[13] D. Han, K. Liu, X. Chen, B. Li, T. Zhai, L. Liu, and D. Shen, "Performance enhancement of a self-powered solar-blind UV photodetector based on $ZnGa_2O_4$/Si heterojunction via interface pyroelectric effect," *Appl. Phys. Lett.*, vol. 118, no. 25, Jun. 2021, Art. no. 251101, doi: 10.1063/5.0049747.

[14] Y. Zhu, K. Liu, Q. Ai, Q. Hou, X. Chen, Z. Zhang, X. Xie, B. Li, and D. Shen, "A high performance self-powered ultraviolet photodetector based on a p-GaN/n-ZnMgO heterojunction," *J. Mater. Chem. C*, vol. 8, no. 8, pp. 2719–2724, Feb. 2020, doi: 10.1039/c9tc06416h.

[15] S. Daimary, P. Chetri, and J. C. Dhar, "High performance UV—A detector using axial n-ZnO/p-CuO p-n junction heterostructure nanowire arrays," *IEEE Electron Device Lett.*, vol. 43, no. 6, pp. 898–901, Jun. 2022, doi: 10.1109/led.2022.3169060.

[16] S. Nakagomi, T. Sakai, K. Kikuchi, and Y. Kokubun, "β-Ga_2O_3/p-type 4H-SiC heterojunction diodes and applications to deep-UV photodiodes," *Phys. Status Solidi A*, vol. 216, no. 5, Mar. 2019, Art. no. 1700796, doi: 10.1002/pssa.201700796.

[17] M. Zhang, Z. Liu, L. Yang, J. Yao, J. Chen, J. Zhang, W. Wei, Y. Guo, and W. Tang, "High-temperature reliability of all-oxide self-powered deep UV photodetector based on ϵ-Ga_2O_3/ZnO heterojunction," *J. Phys. D, Appl. Phys.*, vol. 55, no. 37, Sep. 2022, Art. no. 375106, doi: 10.1088/1361-6463/ac7d1c.

[18] Y.-C. Chen, Y.-J. Lu, C.-N. Lin, Y.-Z. Tian, C.-J. Gao, L. Dong, and C.-X. Shan, "Self-powered diamond/β-Ga_2O_3 photodetectors for solar-blind imaging," *J. Mater. Chem. C*, vol. 6, no. 21, pp. 5727–5732, 2018, doi: 10.1039/c8tc01122b.

[19] D. Zhang, W. Lin, S. Liu, Y. Zhu, R. Lin, W. Zheng, and F. Huang, "Ultra-robust deep-UV photovoltaic detector based on graphene/$(AlGa)_2O_3$/GaN with high-performance in temperature fluctuations," *ACS Appl. Mater. Interfaces*, vol. 11, no. 51, pp. 48071–48078, Dec. 2019, doi: 10.1021/acsami.9b18352.

[20] T.-H. Chou, T.-W. Kuo, C.-Y. Lin, and F.-S. Lai, "A low cost n-SiCN/p-PS/p-Si heterojunction for high temperature ultraviolet detecting applications," *Sens. Actuators A, Phys.*, vol. 279, pp. 462–466, Aug. 2018, doi: 10.1016/j.sna.2018.06.050.

[21] F. Du, Q. Song, X. Tang, Z. Zhang, H. Yuan, C. Han, C. Zhang, Y. Zhang, and Y. Zhang, "Demonstration of high-performance 4H-SiC MISIM ultraviolet photodetector with operation temperature of 550 °C and high responsivity," *IEEE Trans. Electron Devices*, vol. 68, no. 11, pp. 5662–5665, Nov. 2021, doi: 10.1109/TED.2021.3113296.

[22] S. Hou, P.-E. Hellstrom, C.-M. Zetterling, and M. Ostling, "550 °C 4H-SiC p-i-n photodiode array with two-layer metallization," *IEEE Electron Device Lett.*, vol. 37, no. 12, pp. 1594–1596, Dec. 2016, doi: 10.1109/LED.2016.2618122.

[23] F. Juang, Y. Fang, Y. Chiang, T. Chou, and L. ChengI, "A high-performance n-i-p SiCN homojunction for low-cost and high-temperature ultraviolet detecting applications," *IEEE Sensors J.*, vol. 11, no. 1, pp. 150–154, Jan. 2011, doi: 10.1109/JSEN.2010.2052799.

[24] Q. Cai, H. You, H. Guo, J. Wang, B. Liu, Z. Xie, D. Chen, H. Lu, Y. Zheng, and R. Zhang, "Progress on AlGaN-based solar-blind ultraviolet photodetectors and focal plane arrays," *Light, Sci. Appl.*, vol. 10, no. 1, Apr. 2021, doi: 10.1038/s41377-021-00527-4.

[25] J. Yang, K. Liu, X. Chen, and D. Shen, "Recent advances in optoelectronic and microelectronic devices based on ultrawide-bandgap semiconductors," *Prog. Quantum Electron.*, vol. 83, May 2022, Art. no. 100397, doi: 10.1016/j.pquantelec.2022.100397.

[26] C. Lu, Q. Zhang, S. Li, Z. Yan, Z. Liu, P. Li, and W. Tang, "A study for the influences of temperatures on $ZnGa_2O_4$ films and solar-blind sensing performances," *J. Phys. D, Appl. Phys.*, vol. 54, no. 40, Oct. 2021, Art. no. 405107, doi: 10.1088/1361-6463/ac1465.

[27] D. Zhang, Z. Lin, W. Zheng, and F. Huang, "Pt/$ZnGa_2O_4$/p-Si back-to-back heterojunction for deep UV sensitive photovoltaic photodetection with ultralow dark current and high spectral selectivity," *ACS Appl. Mater. Interfaces*, vol. 14, no. 4, pp. 5653–5660, Feb. 2022, doi: 10.1021/acsami.1c23453.